

Fe₂O₃ on patterned fluorine doped tin oxide for efficient photoelectrochemical water splitting

Kwanghyun Kim, Ik-Hee Kim, Ki-Yong Yoon, Jeong-Yeop Lee and Ji-Hyun Jang*

Preparation of patterned FTO (p-FTO)

The FTO substrate was washed by sequential ultrasonication in acetone, isopropanol, deionized water, and ethanol for 10min. each followed by nitrogen blowing. A SU-8 solution (SU-8:CP = 1:2.25) was spin-coated on the cleaned FTO at 3000rpm for 30s followed by prebaking on a hotplate at 100°C for 30min. The photoresist-coated FTO was double-exposed under a 365nm laser source to make square patterns via interference lithography. To determine the pitch distance and the hole diameter of the patterns, the angle of Lloyd's mirror and the time of exposure were varied. The exposed samples were post-baked on the hotplate at 70°C for 10min. The unexposed regions were then removed in a propylene glycol monomethyletheracetate solution for a minute and washed in isopropyl alcohol for 30s, resulting in SU-8 square patterns.

Reactive ion etching (RIE) was performed to vertically etch FTO. The plasma was generated at a pressure of 40mTorr with a RF power of 300W. The gas pressure ratio of CF₄, CHF₃, Ar, and O₂ was around 2:9:1:1. p-FTO was created after removal of the residue of SU-8 by annealing at 500°C for an hour.

Preparation of the α-Fe₂O₃ on p-FTO

The fabrication of the worm-like α-Fe₂O₃ layer followed the procedure previously reported by this group.¹ 30ml of a 150mM FeCl₃ · 6H₂O aqueous solution was transferred into a Teflon-lined autoclave, and the substrates were reclined on the inside of the autoclave facing the p-FTO side to the wall. After 6hrs of reaction at 100°C, a uniform layer of FeOOH was

formed on the p-FTO substrate. The substrates were thoroughly rinsed with D.I. water and ethanol. The samples were then annealed at 550°C in air for one hour to convert FeOOH to a hematite film. To enhance the crystallinity of hematite, the samples were further annealed at 800°C in air for 20min.

Photoelectrochemical measurement

The PEC performance of α -Fe₂O₃ on p-FTO was explored in a three-cell electrode system under front-side illumination of AM 1.5G and 100mW/cm² using 300W power from a Xe lamp. An Ag/AgCl (KCl sat.) electrode and a Pt mesh were used a reference and counter electrode, respectively. A solution of 1M NaOH (pH 13.6) was used as an electrolyte. The exposed area of the working electrode was set to be 0.25cm² by making a window with scotch tape. Photocurrent stability tests were carried out by measuring the photocurrent produced under chopped light irradiation (light/dark cycles of 10s.) at a bias of 1.5V vs. RHE. EIS was carried out at a frequency range from 100kHz to 0.1Hz.

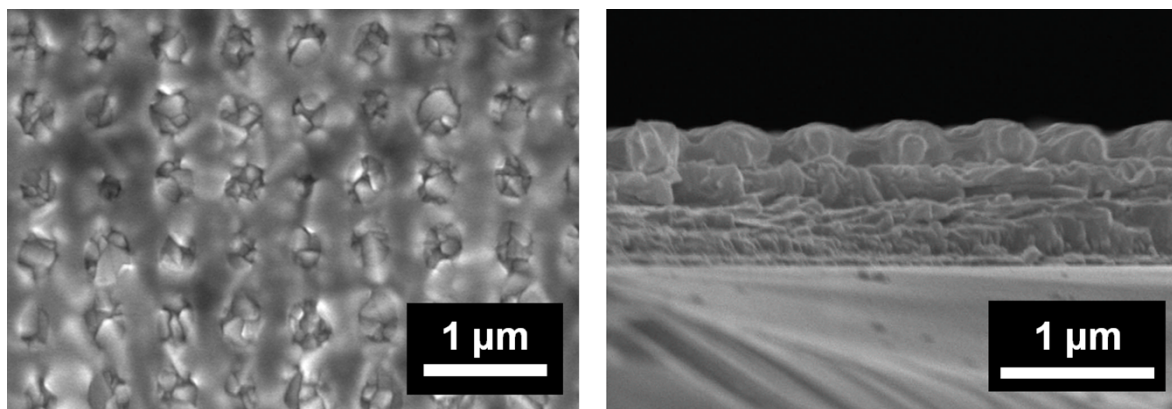


Figure S1. SEM images of SU-8 patterns on FTO; the top view and cross-section view.

The SU-8 layer on the FTO substrate has square patterns with a height of about 300nm and a pitch distance of about 550nm. Its appearance is very important to determine the etched shape of FTO because the RIE passes off vertically.

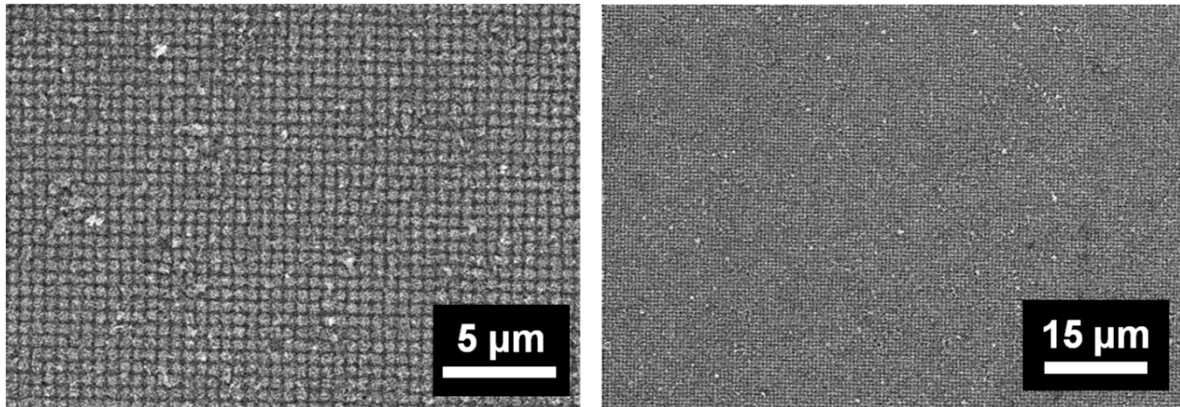


Figure S2. Wide view SEM images of $\text{Fe}_2\text{O}_3/\text{p-FTO}$.

After coating the worm-like hematite layer on p-FTO, a patterned worm-like hematite layer with a periodically well-aligned shape over a very large area was created as shown in **Figure S2**.

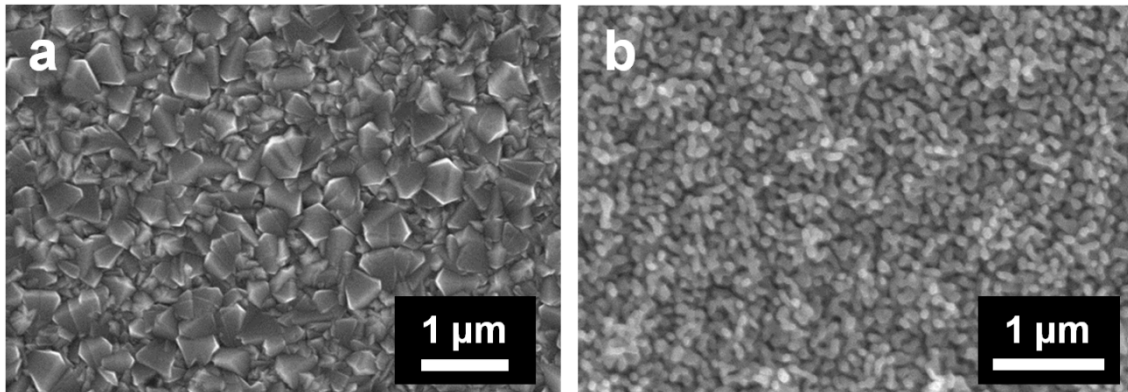


Figure S3. SEM images of a) bare FTO, b) the worm-like shape hematite layer on bare FTO.

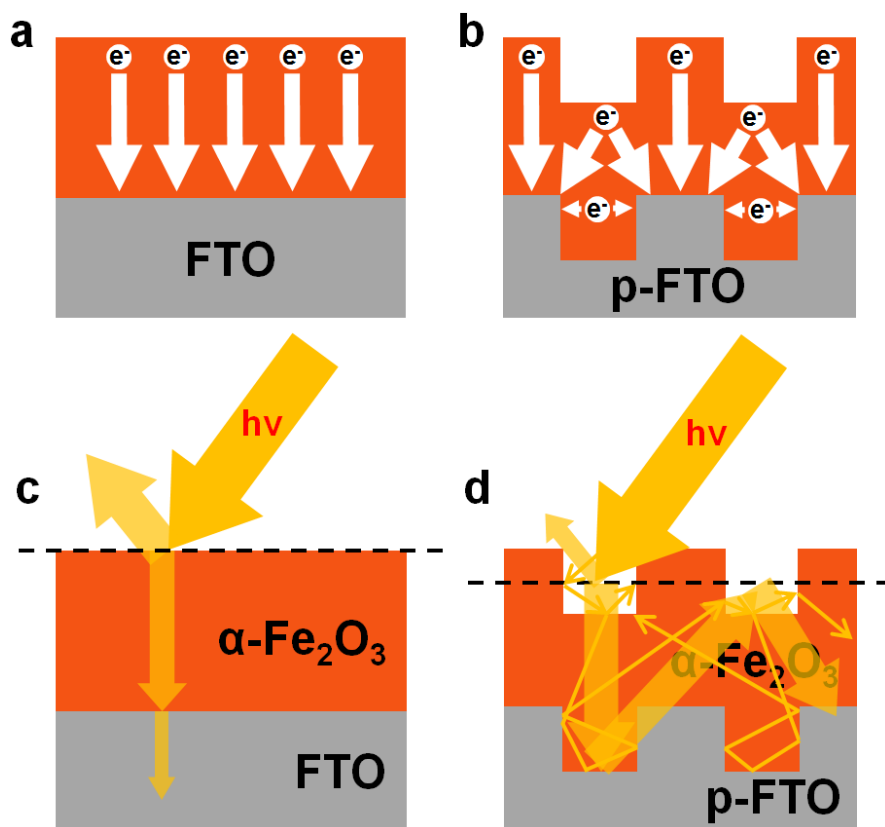


Figure S4. Schematic diagrams that show a), b) the shorter migration pathway of the photogenerated electrons and c), d) the greater scattering of incident sunlight in $\alpha\text{-Fe}_2\text{O}_3/\text{p-FTO}$ than $\alpha\text{-Fe}_2\text{O}_3/\text{bare FTO}$.

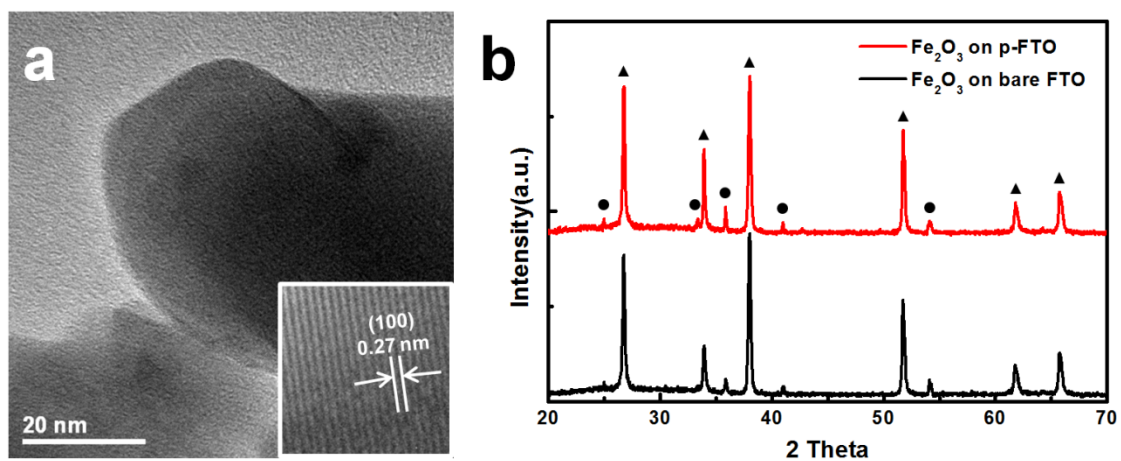


Figure S5. The crystalline hematite material confirmed using TEM and XRD. a) TEM image of the worm-like hematite. The d-spacing in the inset is shown as about 0.27nm

corresponding to the (100) plane of hematite. b) XRD data of Fe_2O_3 on p-FTO and bare FTO. (\blacktriangle indicates the FTO and \bullet is marked at the peaks of hematite.)

The crystallinity of $\alpha\text{-Fe}_2\text{O}_3/\text{FTO}$ and $\alpha\text{-Fe}_2\text{O}_3/\text{p-FTO}$ was investigated by TEM and XRD. d-spacing of about 0.27nm in the inset image in **Figure S5a** confirms the presence of hematite and **Figure S5b** presents proper peaks corresponding to the hematite of $\alpha\text{-Fe}_2\text{O}_3$.

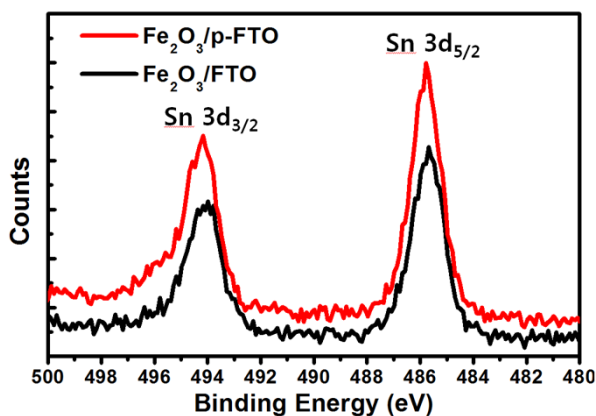


Figure S6. XPS spectra of Sn 3d core levels of the $\text{Fe}_2\text{O}_3/\text{p-FTO}$ and $\text{Fe}_2\text{O}_3/\text{FTO}$.

XPS depth profiles of $\alpha\text{-Fe}_2\text{O}_3/\text{FTO}$ and $\alpha\text{-Fe}_2\text{O}_3/\text{p-FTO}$ were obtained in order to check the possibility of Sn doping. Sn doping onto FTO occurred during high temperature annealing step (800°C, 20min.), which was done to enhance the crystallinity of hematite.² $\alpha\text{-Fe}_2\text{O}_3/\text{p-FTO}$ with a larger contact area between $\alpha\text{-Fe}_2\text{O}_3$ and 3D-shaped FTO was slightly more doped with Sn than FTO, which also might permit the positive effect of patterning FTO on PEC performance.

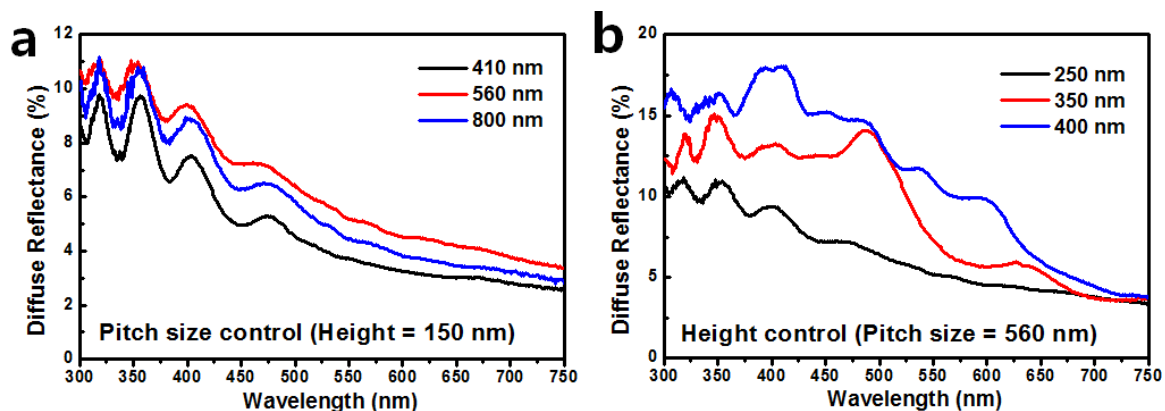


Figure S7. Diffuse reflectance data of a) pitch size and b) height controlled p-FTO samples with fixed the other condition.

We performed diffuse reflectance measurements on p-FTO by varying the pitch size (**Figure S7a**) and height (**Figure S7b**). As can be seen in the diffuse reflectance data, the absorbance of $\text{Fe}_2\text{O}_3/\text{p-FTO}$ with a 560nm of pitch size and a 400nm of height is the greatest, so we optimized the p-FTO with those parameters.

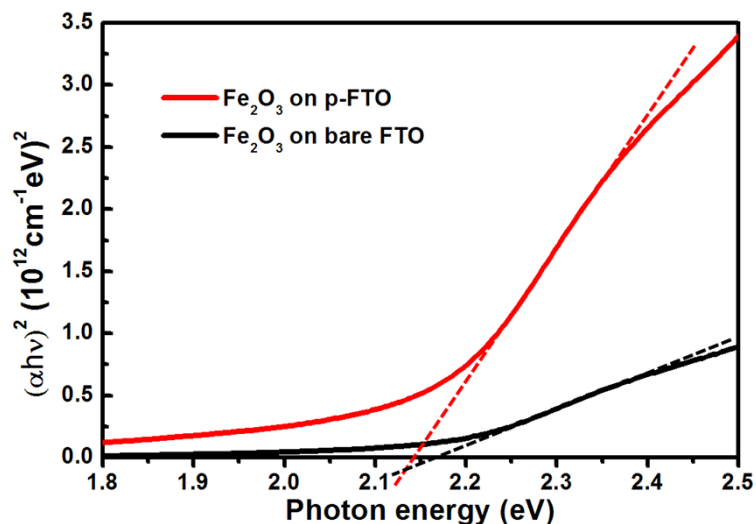


Figure S8. Tauc plots calculated using absorbance data of UV-visible spectroscopy.

The band gap energy of α -Fe₂O₃/FTO and α -Fe₂O₃/p-FTO was obtained by a Tauc plot, which was calculated through the absorbance data in **Figure 2b**.³ **Figure S8** shows that band gap energy of about 2.14eV and 2.17eV was obtained for α -Fe₂O₃/FTO and α -Fe₂O₃/p-FTO, respectively. This value is consistent with the well-known band gap energy of hematite.

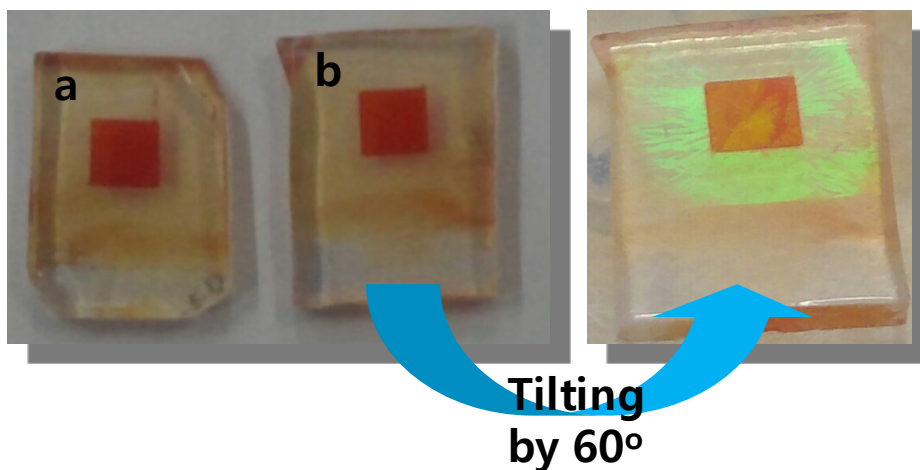


Figure S9. Digital camera image of α -Fe₂O₃/FTO(a) and α -Fe₂O₃/p-FTO(b).

The rainbow color in the background of α -Fe₂O₃/p-FTO with a tilted angle of incident light indicates the presence of the periodic patterns on the surface of FTO.

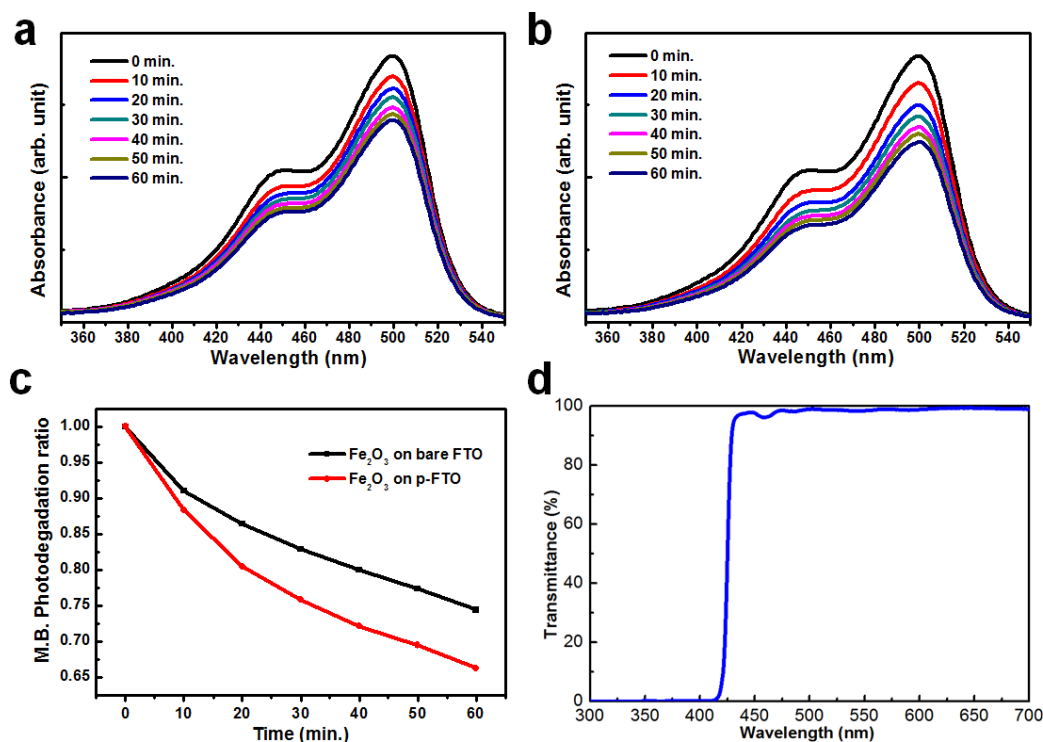


Figure S10. Methylene blue photodegradation ratio for the case of $\alpha\text{-Fe}_2\text{O}_3/\text{FTO}$ and $\alpha\text{-Fe}_2\text{O}_3/\text{p-FTO}$ under visible light illumination ($\lambda > 420\text{nm}$) using a UV cutoff filter. Absorbance data of the methylene blue solution during photodegradation of a) $\alpha\text{-Fe}_2\text{O}_3/\text{FTO}$ and b) $\alpha\text{-Fe}_2\text{O}_3/\text{p-FTO}$. c) Photodegradation ratio of MB for 60min. d) Transmittance data of used UV cutoff filter.

Figure S10 shows the photocatalytic effect of $\alpha\text{-Fe}_2\text{O}_3/\text{FTO}$ and $\alpha\text{-Fe}_2\text{O}_3/\text{p-FTO}$ confirmed via photodegradation of methylene blue ($2.7 \times 10^{-5}\text{M}$). The absorbance peak of methylene blue appears in the region from 350nm to 550nm wavelength. 10ml solutions with $\alpha\text{-Fe}_2\text{O}_3/\text{FTO}$ and $\alpha\text{-Fe}_2\text{O}_3/\text{p-FTO}$ in 20ml vial were shone under visible light via a UV cutoff filter. **Figure S10c** shows the enhanced visible light photocatalytic property of $\alpha\text{-Fe}_2\text{O}_3/\text{p-FTO}$, rather than $\alpha\text{-Fe}_2\text{O}_3/\text{FTO}$. As shown in **Figure S10d**, the wavelength of applied visible light was longer than 420nm. The absorbance curves of the two solutions were checked every 10min.

	Sheet resistivity [Ohm / square]	Thickness [nm]	Resistivity [Ohm · cm]
α -Fe ₂ O ₃ on bare FTO	12.08	1427	1.72 x 10 ⁻³
α -Fe ₂ O ₃ on p-FTO	10.87	1265	1.38 x 10 ⁻³

Figure S11. The electrical conductivity of α -Fe₂O₃/FTO and α -Fe₂O₃/p-FTO confirmed via 4-probe measurement.

References

1. H.-J. Ahn, M.-J. Kwak, J.-S. Lee, K.-Y. Yoon and J.-H. Jang, *Journal of Materials Chemistry A*, 2014, 2, 19999-20003.
2. J. Y. Kim, G. Magesh, D. H. Youn, J.-W. Jang, J. Kubota, K. Domen and J. S. Lee, *Sci. Rep.*, 2013, 3.
3. J. Tauc, R. Grigorovici and A. Vancu, *physica status solidi (b)*, 1966, 15, 627-637.